New Routes to the Characterization and Prediction of Polymer Blend Properties

Michael Tambasco and Jane E. G. Lipson*

Department of Chemistry, Burke Laboratories, Dartmouth College, Hanover, New Hampshire 03755

Julia S. Higgins

Department of Chemical Engineering and Chemical Technology, Imperial College, University of London

Received July 5, 2004; Revised Manuscript Received September 10, 2004

ABSTRACT: Using small-angle neutron scattering (SANS) results, pressure−volume−temperature (*PVT*) data from both polymer melts and blends, and experimentally determined critical temperatures, we employ the lattice Born−Green−Yvon (BGY) theory in the development of new routes for the characterization of polymer fluids and polymer blends. In particular, we focus on blends of polystyrene (PS) with poly(vinyl methyl ether) (PVME) and tetramethylbisphenol A polycarbonate (TMPC). In the first part of the paper we use the analytic expressions derived from the lattice BGY theory to fit the experimental data via three separate routes, using the different kinds of experimental data. In the second part of the paper we investigated the extent to which each of the methods lead to a thermodynamically consistent picture of the blend. Among other findings, we conclude that it is possible to use a relatively sparse data set and still produce a quantitative description of both pure component and blend behavior.

1. Introduction

Making connections between the microscopic nature of a system and its bulk properties has been the driving force for much work in the condensed matter community. Progress in this broad area requires collaboration between theory and experiment with the ideal scenario being a tractable, sophisticated theory applied to the analysis and understanding of the minimum amount needed of easily available, high-quality experimental data. In this paper we report on the progress we have made advancing toward this goal, with our focus being on polymer blends.

On the theoretical side, we make use of a mean-field theory, the lattice Born−Green−Yvon (BGY) theory developed by Lipson and co-workers.[1−7] This approach yields analytic expressions for the free energy and its derivatives which involve a well-defined set of microscopic "characteristic" parameters. The fact that we keep compressibility in the description means that we should not be reducing the energetic interactions to a single parameter. Characterization of the blend therefore requires specifying the lattice size, both of the pure component interaction energies (and effective molecular weights) as well as a mixed interaction energy. If we regard a limiting equation of state description to require no parameters, we end up with something like the ideal gas law: useful in one limit but otherwise uninformative. More sophisticated, but still unsatisfying in terms of predictive power, is a simple theory such as Flory−Huggins (FH).[8] To most this means the well-known lattice random-mixing theory for an incompressible system, with its parameters characterizing lattice size, molecular weights, and energetics, the last through the chi parameter.[9] A simple step forward in complexity yields the compressible version of Flory−Huggins, sometimes known as lattice fluid (LF) theory.[10] The BGY theory is further along this trajectory, in that it naturally includes the effects of nonrandom mixing, and it also is able to incorporate nearest-neighbor connectivity. The theory developed by Panayiotou and Vera[11] also makes progress in this direction, and it as well as the Flory−Huggins and lattice fluid theories may all be obtained from the BGY theory by taking suitable limits.[5]

On the experimental side there are many kinds of data available for polymer blends, but those most commonly used in applying BGY and many other theories have been coexistence curve results and, for characterization of the pure components, pressure−volume−temperature (*PVT*) data. This approach has yielded useful and interesting results, yet it remains unsatisfactory in several ways. For one thing, the mixed interaction energy of the blend is typically obtained by fitting to the critical point, that is, the single point on the coexistence curve which is *not* well-described by a mean-field theory. In addition, this route limits applications to those systems for which *PVT* data are available for the pure components. While the literature does contain such results, it would be liberating to be able to study mixtures of polymers one or both of which have not been particularly well-characterized.

In this paper we describe two new routes for combining experimental data and the BGY theory to the study of polymer blends. For both of these routes, we obtain optimized characteristic parameters for both components as well as the blend from one data set. We chose two very well-studied mixtures: polystyrene blended with poly(vinyl methyl ether) (PS/PVME)[12−15] and PS blended with tetramethylbisphenol A polycarbonate (TMPC).[12,16−18] In light of the closing remark in the last paragraph, this choice seems somewhat perverse. However, since the analyses described here are new, it is critical that they be compared with results using widely applied methods. The older route (the "pure/LCST" route) involves *PVT* data for the pure components and then analysis of a single temperature; each blend in this work exhibits a lower critical solution temperature (LCST). For one of the new routes, the "mix route", we make use of blend *PVT* data, two compositions for each

10.1021/ma048647h CCC: $27.50
Published on Web 11/03/2004

blend. These *PVT* data are fit to obtain all of the characteristic parameters needed, for both the pure components and the mixture. The second new route, the "NS route", makes use of zero-angle scattering intensities (from neutron scattering (NS) measurements) as a function of temperature. Even without knowing how well the two new routes do, we anticipate that the SANS method will attract more interest because these measurements yield a wealth of additional information about mixtures.

In section 2 we provide experimental and theoretical background. Section 3 provides a description of the fitting procedures. The BGY predictions are presented in section 4, and in section 5 we summarize and conclude.

2. Experimental and Theoretical Background

Experiment. With the exception of the neutron scattering studies on the polystyrene (PS)/tetramethylpolycarbonate (TMPC) blend, all of the experimental results were obtained from the literature. Details concerning the measurements on polystyrene (PS) and poly(vinyl methyl ether) (PVME) and their mixtures may be found in refs 12 and 13. The *PVT* data for PS, TMPC, and blends of the two are available in ref 16. In ref 12, a very useful compendium of *PVT* data, the results are presented as specific volume as a function of temperature, at fixed pressures. The absolute accuracy of the specific volume measurements is given as 0.002 cm^3/g, and the pressures are said to be constant to within 0.1 MPa.

The data for the coexistence curves which we have used here have all been obtained from light scattering experiments. When a blend system becomes two-phase, light is scattered as long as two conditions are fulfilled. These are that the refractive indices of the two polymers are sufficiently different—a condition obeyed by both the blends reported—and that the developing phases are comparable in size to the wavelength of light. This second condition is not always obeyed in the early stages of phase separation.[19] In typical experiments initially homogeneous samples are heated at a steady rate until the cloud point is detected either by a reduction in the transmitted light or by an increase in the scattered light. If the initial phase size is small, an apparent lag can occur before the cloud point is detected, which results in a cloud point temperature higher than reality. Such a lag can also occur if the system is very close to the glass transition temperature so that molecular motion is slow compared to the heating rate. In either case the problem is dealt with by observing the cloud points at decreasing heating rates and extrapolating to zero rate. Such extrapolation is reported in refs 13 and 14 for the PS/PVME and dPS/PVME cloud point results and in ref 18 for the PS/TMPC experiments.

One further potential complication of interpreting the coexistence data should be mentioned. The samples are heated from the one phase region, and except at the critical composition, they must pass first the binodal and then the spinodal. The question then arises as to which corresponds to the cloud point temperatures reported. The processes of nucleation and growth which govern phase separation in the metastable gap between spinodal and binodal are very much slower than spinodal decomposition. Thus, it is likely and has been confirmed in some cases where the spinodal was obtained directly (by extrapolation of the spinodal decomposition rate following temperature jump experiments inside the spinodal boundary) that the cloud point is closer to the spinodal than to the binodal. This is true for high molecular weight blends where molecular motion is slow and for compositions close to the critical values. For compositions well away from critical, however, where the metastable gap becomes very wide, the cloud points may well fall between binodal and spinodal curves.

Table 1. Pure Component Parameters for Several Data Types

polymer	M_w (g/mol)	ϵ_{11} (J/mol)	$v \times 10^3$ (L/mol)	r	notes
PS[12]	110 000	−2245.6	9.197	10162.6	pure *PVT* data
PS[16]	253 000	−2115.3	9.115	21499.4	pure *PVT* data
PS[12]	114 200	−2228.2	9.504	10640	blend *PVT* data
PS[16]	253 000	−2133.1	9.38	21126.8	blend *PVT* data
PS[15]	225 000	−2105.5	9.9	19071.1	NS data
PS[18]	250 000	−2251.1	9.5	22301.1	NS data
PVME[12]	99 000	−2044.1	9.467	9393.9	pure *PVT* data
PVME[12]	99 000	−1982.9	9.504	9175.1	blend *PVT* data
PVME[15]	99 000	−2000.9	9.5	9287.7	NS data
TMPC[16]	42 000	−2225.3	10.78	3458.1	pure *PVT* data
TMPC[16]	42 000	−2216.3	9.38	4722.9	blend *PVT* data
TMPC[18]	54 000	−2209.5	9.9	4390.8	NS data

Information about the molar masses of the polymers is listed in Table 1, along with characteristic parameters obtained by a variety of different routes, as described in the next section.

The neutron data presented here were obtained using the PAXE spectrometer located at the Orphee reactor in Saclay France.[18] Scattering data were obtained from samples equilibrated at the measurement temperature in a q range $0.008 < q < 0.078$ $Å^{-1}$. This corresponds to a mean incident wavelength of 6 Å and a sample−detector distance of 5 m. The samples were prepared from solutions in toluene at 10% w/v which had been cast as thin films onto glass and dried under vacuum for 4 weeks at increasing temperature, finally reaching T_g plus 20 °C. Ten of these thin films were then stacked together and wrapped in aluminum foil to give a sample of thickness 1 mm. Extremely careful data treatment is described in detail in ref 18 to remove background scattering and to achieve intensities normalized to an absolute scale. In particular, great care was taken to ensure that the samples had properly equilibrated at the measurement temperature.

This care and attention is worth discussing here as it provides assurance for the reliability of the data used to fit the model calculations. The need for careful analysis of the neutron experimental data in terms of background subtraction, transmission corrections, and sample thickness normalization is important. Particular problems which can be identified are incomplete annealing and/or too slow a quench process in cases where the SANS experiments are to be carried out at ambient temperature.

The SANS data for PS/PVME are taken from ref 15. In a journal paper it is not possible to report at the same level of detail as in a doctoral thesis. As a consequence the confidence in the data has to be based at least in part on the reputation of the research group involved and of the neutron source used. In the case of ref 15 these are both high. The reported method of sample preparation is very close to that described above for the PS/TMPC data. The data analysis is likely to have been as careful, but this has to be taken somewhat on trust. Confidence is given by the good correspondence between the neutron cloud points and those obtained by light scattering.

Theory. This research uses the results of the lattice Born−Green−Yvon (BGY) theory,[4] applied to a simple cubic lattice having coordination number, z, equal to six. The total lattice volume is represented by $V = v(N_0/N_A)$, where v is the volume per mole of lattice sites, N_0 is the total number of lattice sites, and N_A is Avogadro's number. The parameter r_i represents the number of contiguous lattice sites occupied by a molecule of species i. For a binary mixture (where $i = 1, 2$) the site fractions are defined as $\phi_i = r_i N_i/N_0$, $\phi_h = N_h/N_0$, and $\phi = 1 - \phi_h$, where N_i is the total number of molecules of i and N_h is the number of unoccupied lattice sites (or holes). The maximum number of interaction sites available to a molecule of component i is given by $q_i z = r_i(z - 2) + 2$. This leads to the definition of concentration variables $\xi_i = q_i N_i/(N_h + \sum_j q_j N_j)$ and $\xi_h = N_h/(N_h + \sum_j q_j N_j)$ which account for the molecule's nearest-neighbor connectivity. The interaction energy of nonbonded nearest neighbors of the same species is given by ϵ_{ii}, while unlike nearest-neighbor interactions are denoted by ϵ_{ij}. The BGY integral equation hierarchy links distribution functions at successively higher order. In the lattice BGY theory derived by Lipson and co-workers the hierarchy is closed off at the level of pair interactions via the Kirkwood superposition approximation; the independence approximation is used for all pair functions except the pair of interest. Expressions for the probability of the different types of nearest-neighbor contacts are detailed in ref 9. An analytic expression for the internal energy of the system is derived by summing the product of these probabilities multiplied by the associated energetic contribution. As noted above, use of the site fractions account for local chain connectivity. Each component is characterized by specifying values for the characteristic parameters ϵ, r, and v. Since the systems are compressible at finite (experimental) pressures, all of the interaction energies contribute to the blend's internal energy. The temperature dependence of this energy allows for the determination of an analytic expression for the free energy using a Gibbs−Helmholtz relationship. This relationship mandates the use of an entropic approximation for infinite temperature, and we make use of the Guggenheim result.[20] The system is taken to be randomly mixed only at infinite temperature, while at finite temperatures the BGY theory yields nonrandom contributions to the entropy of the mixture. The BGY result for the dimensionless configuration Helmholtz free energy, $\hat{a}$, of a K-component blend is given by

$$\hat{a} = \sum_{i=h,1}^{K} \left(\frac{\phi_i}{r_i} \ln \phi_i + \frac{q_i z \phi_i}{2 r_i} \left\{ \ln\left[\frac{\xi_i}{\phi_i}\right] - \ln[\xi_h + \sum_{j=1}^{K} \xi_j \exp(-\beta \epsilon_{ij})] \right\} \right) \quad (1)$$

where $\beta = 1/(k_B T)$, k_B is Boltzmann's constant, and T is the temperature. Accordingly, the Helmholtz free energy density, A/VT, is given by

$$A/VT = k_B \hat{a}/v + a_0 \quad (2)$$

where a_0 is a caloric background not needed in this work. The blend's thermodynamic properties can then be obtained from this derivative of the Helmholtz free energy density

$$\mathrm{d}(A/VT) = \frac{U}{V} \mathrm{d}(1/T) + \sum_{j=1}^{K} \frac{\mu_j}{T} \mathrm{d}(\rho_j) \quad (3)$$

where U is the internal energy of the system, r_j is the number density of component i, and μ_j is the chemical potential of species i. The chemical potential for component i is given by

$$\mu_i = \frac{r_i}{\beta} \left(\frac{\partial \hat{a}}{\partial \phi_i} \right)_{\beta, \varphi_{k \neq i}} \quad (4)$$

The chemical potential difference between the blend components may be used to either fit or predict neutron scattering intensities. This is accomplished by correlating the BGY expression for the chemical potential to the value used in neutron scattering analyses. The relationship describing the scattering intensity is given by[21]

$$I(q=0) = \langle b \rangle [S(0)] \langle b \rangle^T \quad (5)$$

where $I(q=0)$ is the zero-angle scattering intensity, $S(0)$ is the dynamic structure factor, and $\langle b \rangle$ and $\langle b \rangle^T$ are evaluations of the matrices for the scattering lengths of the sample. The T superscript is indicative of the column evaluation of the matrix, while a lack of superscript indicates an evaluation of the data along the row. There are two possible types of interactions between an incident neutron wave and the scattering sample. These two types are *coherent* and *incoherent* scattering. If all incident waves demonstrate identical interaction with the scattering system, the phase shifts will be the same and the interference effects are denoted as coherent.[21] Coherently scattered waves yield information concerning atomic positions. However, if no correlation of the incident waves exists within the scattering system, the interaction potential of the system will fluctuate randomly about an average value (denoted by the symbol $\langle V \rangle$). These variations arise from isotropic incoherence and neutron/nucleus spin interactions. Thus, given the nature of polymer systems, the incoherent scattering contribution is treated as background noise and subtracted from the total scattering intensity values. Considering a two-component system, eq 5 may be expanded to give

$$\frac{I(q=0)}{V} = \left(\frac{b_2}{v_2} - \frac{b_1}{v_1} \right)^2 \frac{k_B T \varphi}{-v_0 \dfrac{S^{-1}(0)}{k_B T}} \quad (6)$$

where V is the total sample volume and b (for components 1 and 2) are the component's associated scattering lengths. The v values (with subscripts 1 and 2) are the monomer molar volume for each component. The symbol v_0 is the geometric average of the molar volumes. Generally, b is a complex quantity whose value depends on the orientation and spins of both the neutron beam and the scattering nucleus. The "real" portion of the scattering length may be positive (attractive interactions) or negative (repulsive interactions). The partial derivative of the osmotic compressibility (π) with respect to volume fraction (φ) may be substituted for the structure factor, yielding

$$\frac{I(q=0)}{V} = \left(\frac{b_2}{v_2} - \frac{b_1}{v_1}\right)^2 \frac{k_B T \varphi}{\frac{\partial \pi}{\partial \varphi}} \tag{7}$$

After substituting according to the relationship $\partial\pi/\partial\phi = -v_0(\partial\mu/\partial\phi)$, the final expression correlating the chemical potential to the zero-angle scattering intensity is given by

$$\frac{\partial \mu}{\partial \varphi} = V\left(\frac{b_2}{v_2} - \frac{b_1}{v_1}\right)^2 \frac{k_B T \varphi}{-v_0 I(q=0)} \tag{8}$$

The phase transitions for binary mixtures are usually represented in terms of the molar density ($\rho = \rho_1 + \rho_2$) and mole fraction ($x = \rho_2/\rho$). Conjugate to the mole fraction is the difference between the component's respective chemical potential (where $\mu = \mu_2 - \mu_1$). These terms allow for the critical conditions to be expressed by[22]

$$\left(\frac{\partial \mu}{\partial x}\right)_{T,P} = 0, \quad \left(\frac{\partial^2 \mu}{\partial x^2}\right)_{T,P} = 0 \tag{9}$$

where the initial expression defines the spinodal line and the second equation defines a critical point as an extremum of the spinodal. Thus, the lower critical solution temperature (LCST) represents the minimum of the spinodal (and conversely, the upper critical solution temperature, or UCST, represents the maximum). Hence, for a pressure P, the coexisting phases satisfy the expressions $\mu(T,P,x_1) = \mu(T,P,x_2)$ and $\mu_1(T,P,x_1) = \mu_1(T,P,x_2)$.

In this work we use three distinct routes in fitting experimental data to determine the characteristic parameters. One of the three is the familiar path involving a fit to pure component *PVT* data in order to obtain the pure component characteristic parameters, followed by a fit to the blend critical temperature in order to characterize the mixed interaction. The other two routes involve using experimental data on the blend alone, obtained either from neutron scattering experiments or from *PVT* measurements on the mixture. The fitting procedure for these two routes yields all of the pure species and blend parameters at once. In all cases we characterize the mixed interaction energy by using the parameter g

$$\epsilon_{12} = g(\epsilon_{11}\epsilon_{22})^{1/2} \tag{10}$$

3. Fitting of Experimental Data

Pure Components. The route we have followed in all previous studies of polymer mixtures involved fitting the BGY equation of state (the form shown here is for a one-component fluid)

$$P = -\frac{1}{\beta v}\left\{\ln \phi_h + \frac{z}{2}\ln\left(\frac{\xi_h}{\phi_h}\right) + \phi\left(1 - \frac{1}{r}\right) + \frac{z\phi}{2}\left(\frac{q}{r} - 1\right) + \frac{z\xi^2}{2}\left[\frac{\exp(-\beta\epsilon) - 1}{\xi \exp(-\beta\epsilon) + \xi_h}\right]\right\} \tag{11}$$

to experimental pressure−volume−temperature (*PVT*) data so as to obtain values for the characteristic parameters r, v, and ϵ.[23] In this paper one of the three routes used in studying the blends of interest requires that the pure component data be fit. Figure 1 shows the results for PVME (part a) and TMPC (part b), wherein the pressure is plotted as a function of molar volume for a series of temperatures (given in the figure caption). The symbols represent experimental data and the curves show the optimized BGY fit. This figure, which illustrates the ability of the BGY equation of state to capture the experimental *PVT* behavior, is typical of the results obtained for polymeric fluids; analogous results for PS have been recently published.[7] In Table 1 we summarize the characteristic parameters obtained from fitting data for each of the pure polymers. The r values in the table are associated with the molecular weights listed. For a sample of different molecular weight the ϵ and v values would remain the same, and the r value would simply be rescaled so that $r_2 = r_r(MW_2/MW_1)$. Each of the pure fluid *PVT* fits yields a characteristic v

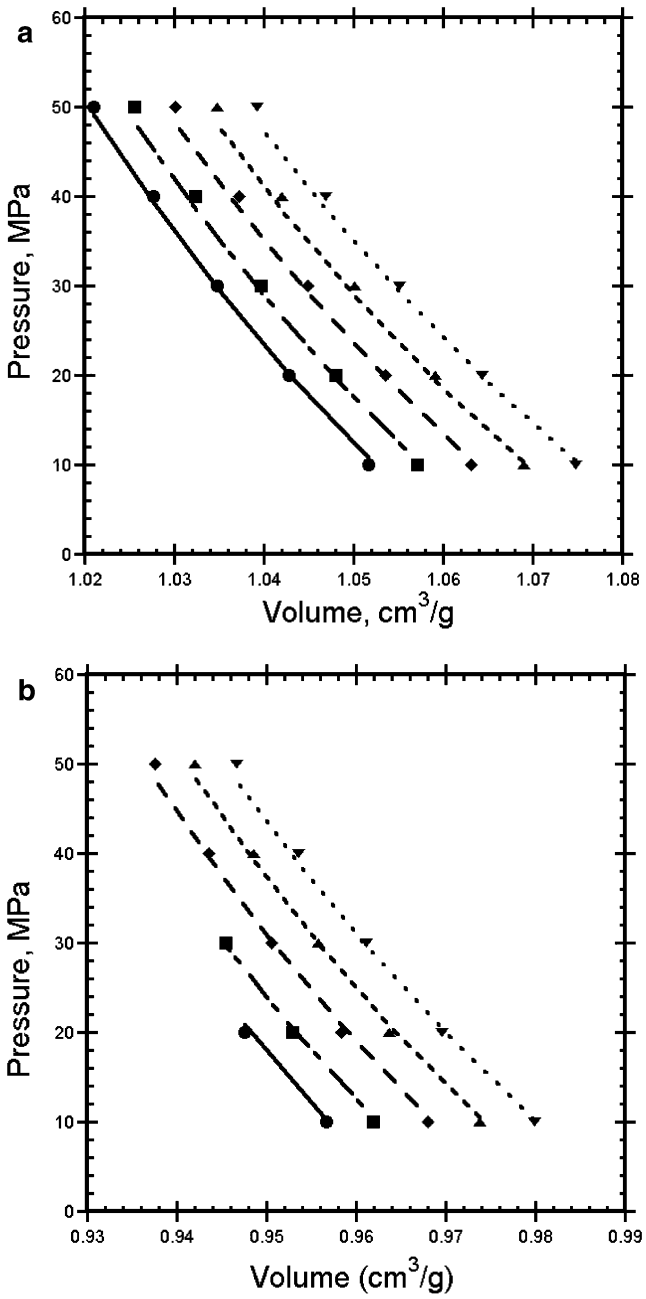

Figure 1. Pressure as a function of molar volume; symbols represent experimental data,[11,15] and the curves show the optimized BGY fit. Temperatures refer to the results from left to right: (a) PVME (438, 447, 455, 464, 473 K); (b) TMPC fit (488, 497, 507, 516, 525 K).

value. However, to avoid having a lattice whose site volumes are composition-dependent, we use a single v value for each of the pure components as well as the blend. There are several routes by which the value of v may be fixed: choosing what appears to be a reasonable value, taking the average of the two pure values, or choosing one of the pure component v values. Once v is fixed, the remaining pure component parameters are reoptimized by refitting the *PVT* data. For all of the results reported here we chose to fix v at the arithmetic average of the individual values obtained through the initial *PVT* fits.

Blends. *Pressure−Volume−Temperature Results.* As noted above, one of the reasons we chose the blends PS/PVME and PS/TMPC was the availability of a wide variety of data. In particular, it is atypical to find *PVT* results for blends. However, for PS/PVME data have been tabulated for nine compositions (from 10% to 90% PS), while for PS/TMPC results have been obtained for two compositions (33% and 67% PS). We restricted our study of the PS/PVME blend to two compositions (30% and 70% PS) so that the analysis for the two blends would be comparable. Figure 2 shows the fit results for PS/PVME to the *PVT* surfaces for 30% PS (part a) and 70% PS (part b). Once again, the plot shows pressure as a function of molar volume for a series of isotherms. Figure 3 depicts the fit results obtained for PS/TMPC for 33% PS (part a) and 67% PS (part b). As these plots demonstrate, the BGY equation of state is equally well-suited to describe both the pure components and the mixtures. In each case, the fit to the combined set of two mixture *PVT* surfaces yields the entire set of parameters, viz. the characteristic parameters of each blend component, a single optimized v, and the g value.

Neutron Scattering Results. As noted earlier, the zero-angle scattering intensity is directly related to the second derivative of the free energy of mixing. As the BGY lattice theory yields an analytic expression for this quantity, it is possible to fit the theoretical equation, which incorporates the characteristic parameters of the pure fluids and the mixture, to experimental data. An equivalent route is to form the partial derivative of the chemical potential (μ) with respect to the volume fraction

$$\frac{\partial \mu}{\partial \varphi} = \sum_{i}^{K} \frac{r_i}{\beta} \left(\frac{\partial^2 \hat{a}}{\partial \varphi_i^2} \right)_{\beta, \varphi_{k \neq i}} \tag{12}$$

where r_i is the characteristic parameter r of component i and $\hat{a}$ is the Helmholtz energy.[11] The experimental constants used in tabulating the zero-angle intensities are summarized in Table 2, along with the optimized pure component and mixture parameters obtained from the different mixture fits described here.

For the PS/TMPC blend scattering intensities have been tabulated for 30%, 50%, and 70% PS. We restricted our analysis to the 50% PS blend because the data were collected over the largest temperature range. Figure 4a shows the experimental data (symbols) and the BGY fit (solid line) for the inverse scattering intensity as a function of the deviation from the critical temperature. The BGY fit is constrained so as to pass through the origin. The analogous results for the PS/PVME blend (50% PS) are shown in Figure 4b and are also constrained to pass through the origin. The characteristic parameters obtained for both blends are listed in Table 2.

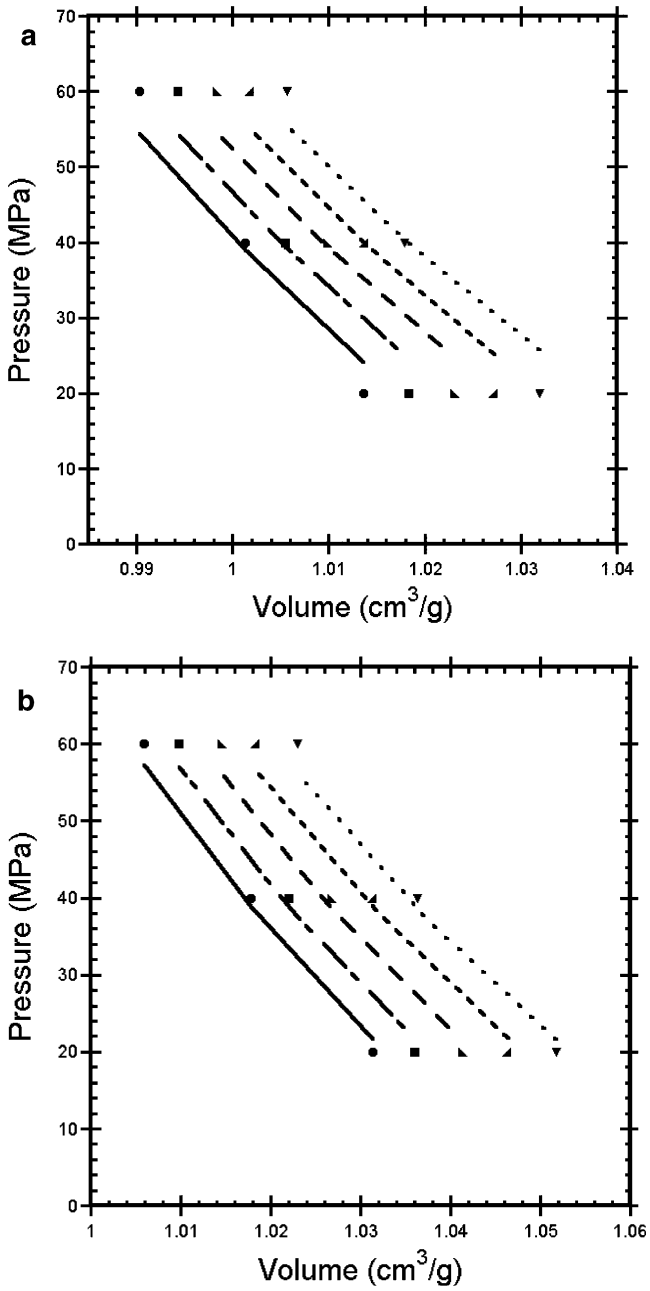

Figure 2. Pressure as a function of molar volume for PS/PVME blend. Symbols represent experimental data,[11] and curves show the optimized BGY fit. (a) 30 wt % PS (359, 367, 375, 382, 391 K); (b) 70 wt % PS (343, 351, 359, 367, 375 K).

Critical Solution Temperatures. In fitting the mixture surface data and the neutron scattering data, it was possible to obtain optimized values for all the required parameters (pure and mixed) by fitting to a limited set of mixture data. Both of these methods represent new routes to the fluid/mixture parameters. In contrast, the third route we use here is the one we have relied upon in the past: fit each of the pure component *PVT* surfaces and then fit to a critical temperature in order to determine a value for g. Here we determine the g parameter by a fit to the lower critical solution temperature only (not the critical composition) of each blend. The coexistence curves shown in Figure 5 are therefore pinned to the LCST, but with the exception of that one temperature the rest of the curve (including the critical composition) represents the BGY prediction. In each

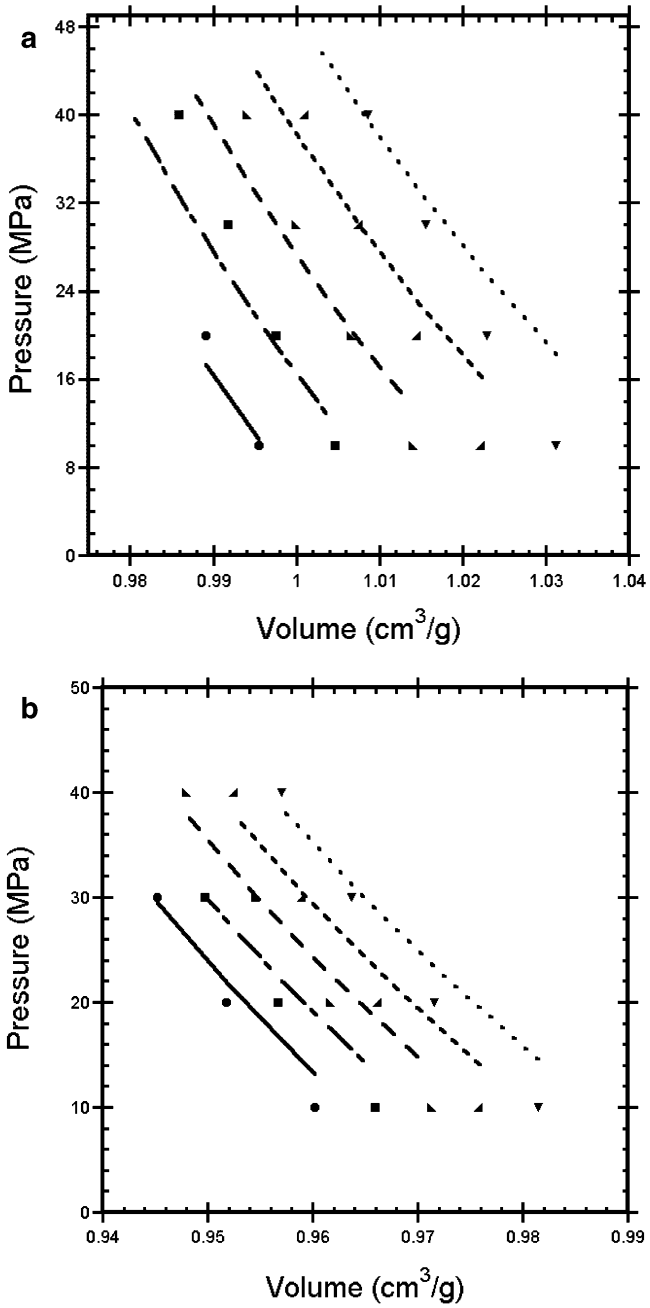

Figure 3. As in Figure 2, for the PS/TMPC blend.[15] (a) 33 wt % PS (416, 431, 446, 461, 476 K); (b) 67 wt % PS (467, 476, 490, 503, 516 K).

Table 2. Blend Parameters for Several Data Types

blend	MW ratio	$v \times 10^3$ (L/mol)	g	notes
PS/PVME[13]	110 000/99 000	9.504	1.001 17	pure fluid +
dPS/PVME[14]	119 000/99 000	9.504	1.001 35	LCST data
PS/TMPC[17]	253 000/42 000	9.857	1.000 359	
PS/PVME	114 200/99 000	9.504	1.001 92	blend *PVT*
PS/TMPC	253 000/42 000	9.38	1.000 148	data
PS/PVME	250 000/99 000	9.5	1.002 3	neutron
PS/TMPC	225 000/54 000	9.9	1.000 28	scattering data

case the filled symbols represent the experimental data, the calculated spinodal curve is represented by the dotted line, and the solid line shows the predicted binodal curve. Figure 5a shows the results for the PS/PVME blend, while those for PS/TMPC are shown in Figure 5b. The parameters determined from the critical temperature fits are tabulated in Table 2.

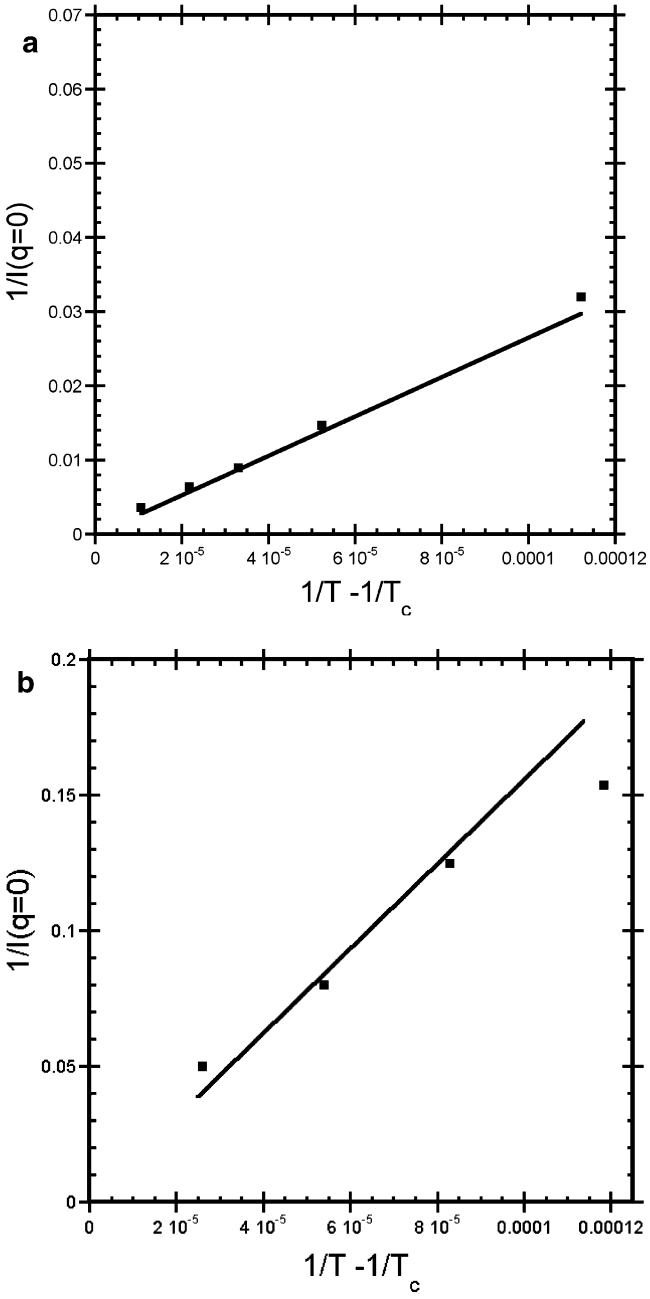

Figure 4. Inverse zero-angle scattering intensity as a function of inverse temperature for (a) PS/TMPC (50 wt % PS) and (b) PS/PVME blend (50 wt % PS). The symbols represent experimental data,[14,17] and the line is the BGY fit.

4. Comparison of Predicted Blend Behavior with Experimental Results

Pressure−Volume−Temperature Surfaces. Prediction of the *PVT* surface of a blend is a demanding test of a theory in that it involves behavior as a function of four variables: pressure, volume, temperature, and composition. In the cases discussed here there are further complications associated with the blend glass transition and critical temperature. For PS/PVME the experimental LCST is about 393 K. The glass transition temperature for pure PS is 373 K, while that for pure PVME is 249 K. We studied the blend *PVT* surface for the two compositions having 30% PS and 70% PS. If

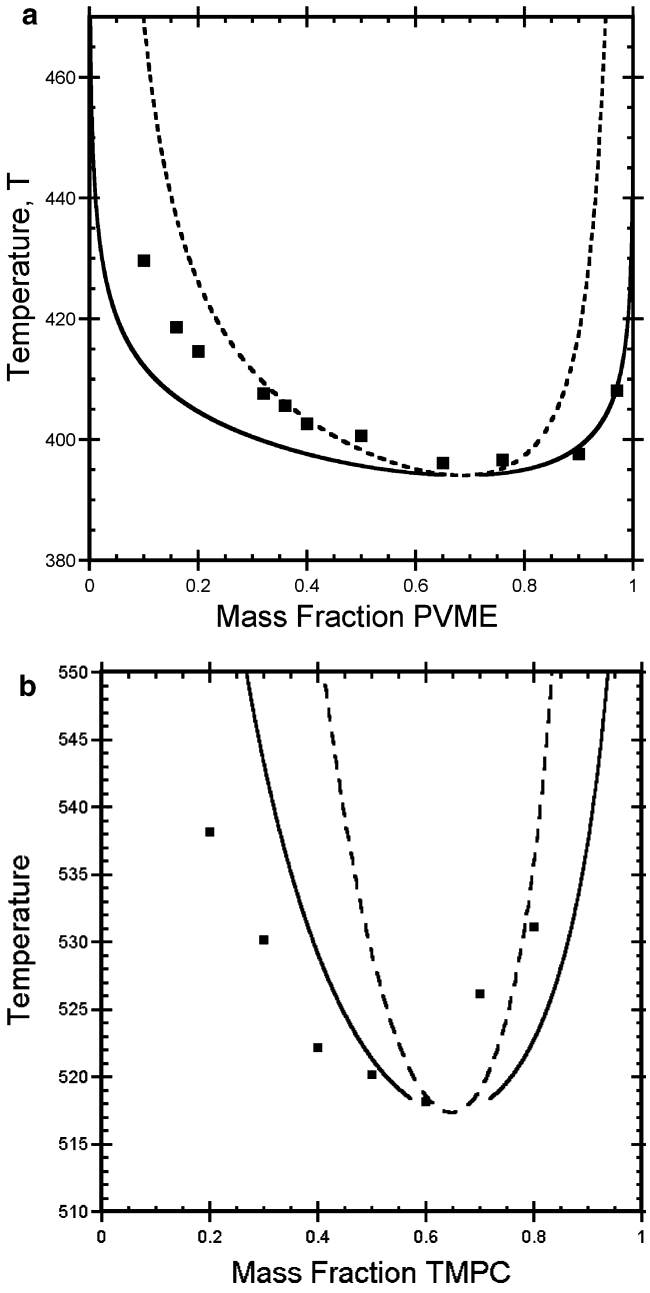

Figure 5. Coexistence results for PS/PVME (a) and PS/TMPC (b). The symbols represent experimental data.[12,16] The curves show the BGY predictions for the binodal and spinodal, where in each case the critical temperature was used to fit for the g parameter, characterizing the mixed interaction energy.

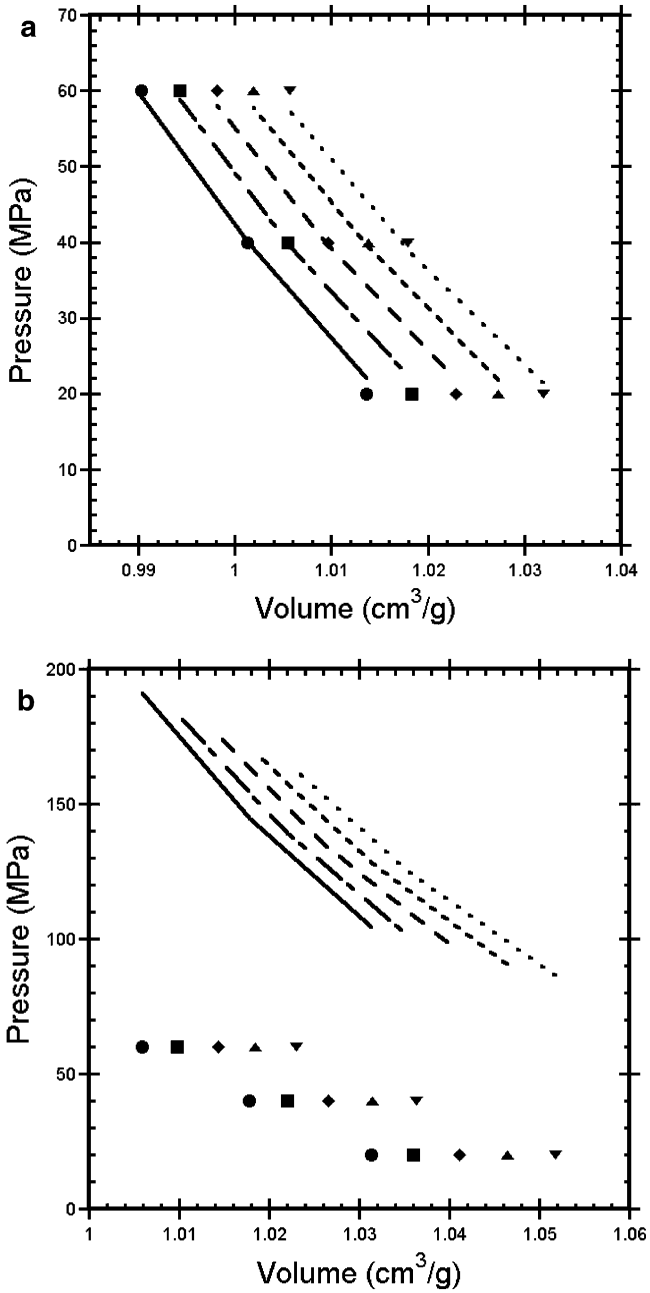

Figure 6. Best and worst of the BGY predictions for the PVT behavior of PS/PVME: (a) for the 30% PS surface using the NS fit parameters (NS route); (b) BGY prediction for the 70% PS surface using the pure/LCST parameters. The symbols represent experimental data.[11]

we estimate the glass transition of the blend by taking a composition-weighted sum of the pure component glass transitions (as is done using the Flory−Fox relationship), this gives an estimate of 286 K for the 30% PS blend and 336 K for the 70% PS blend. In Figure 2, the BGY *fits* to the experimental *PVT* data of the PS/PVME blend are shown. Here, in Figure 6 we see the *predictions* for *PVT* behavior of the blend using the parameters obtained by fitting the neutron scattering data (NS fit) in part (a) and, in a completely separate procedure, the *predictions* using the pure component *PVT* data plus the experimental LCST (pure/LCST fit) in part (b). Each set of parameters was used separately to generate a surface for each of the two compositions. Figure 6 shows only half of the results: the best and the worst. In Figure 6a the NS fit parameters were used to predict the 30% PS surface; in Figure 6b the pure/LCST parameters were used to predict the 70% PS surface. The agreement between prediction and experiment for the former appears to be excellent, while it is very poor for the latter. However, it is relevant to note that the temperature range for the *PVT* data is 300−470 K, which means that for a blend containing 70% PS (as shown in Figure 6b) the glass transition (336 K) and the relevant binodal temperature (roughly 410 K) are both well within the temperature range in which the *PVT* data were collected. This blend therefore is apparently both glassy and phase separated within the temperature range of interest! On the other hand, the parameters that were used to generate both sets of predictions were obtained by fitting data which were taken above the glass transition and below the LCST, where the blend was a one-component melt. Considering

the different sets of circumstances involved, the lack of agreement between prediction and experiment for the 70% blend becomes understandable. The situation for the 30% PS blend (Figure 6a) is not quite so dire as for the 70% PS blend. For the 30% PS blend the estimated glass transition (286 K) is about 14 K below where the *PVT* data begin; this blend surface should therefore all lie in the melt region, although closer to the glass transition than the minimum 50 K difference we prefer to keep when analyzing the pure *PVT* data. On the other hand, a composition of 30% PS is close to the critical composition, and the critical temperature, about 395 K, is in the middle of the *PVT* range. A further complication is that the NS predictions are made using parameters obtained by fitting scattering data for the deuterated-PS blend, while the *PVT* surface is for the hydrogenous-PS blend. Despite all of these issues the NS prediction appears to be in very good agreement with the experimental *PVT* data. It is interesting to note that the NS prediction for the 70% PS surface is in significantly poorer agreement with the data, although not as poor as that shown in part (a) of the figure, while the pure/LCST prediction for the 30% blend is in closer agreement with the data (although not as close as that shown in part (b)). The presence of a glass transition is an important factor in determining how closely the predicted and experimental *PVT* surfaces coincide. This hypothesis is supported by the analogous comparisons made using results for the PS/TMPC blend.

Figure 7 is analogous to Figure 6; in this case the concentrations are 33% PS for the NS prediction shown in part (a) and 67% PS for the pure/LCST prediction shown in part (b). However, for the PS/TMPC blend the predictions using the NS parameters and the pure/LCST predictions are so similar as to be indistinguishable for each of the two compositions, while for PS/PVME the two routes to predicting the *PVT* surface gave very different results. The fact that both phase separation and the glass transition occurred within the temperature range of *PVT* data for the PS/PVME blend is clearly important. In the case of PS/TMPC the lowest temperature for the blend *PVT* data is 475 K, which is about 20 K above the glass transition for TMPC and 100 K above that for PS. However, while the temperature on the binodal for the 67% PS blend is approximately 405 K, putting this mixture well into the one-phase region, which for the 33% PS blend is about 520 K, very close to the blend LCST. Thus, three out of the four *PVT* data sets for this composition are within 20 K of the binodal temperature. This may be correlated with the fact that both the fit to and the prediction of the *PVT* data for this composition are not as close to the experimental data as for the 33% PS composition, where proximity to the binodal is not an issue. One may also deduce some rationale for whether there is "path dependence" in the predictions by looking at differences in the parameters. For both PS and the TMPC the pure/LCST and NS fit values for ϵ differ from the mixture fit value by no more than about 1%. On the other hand, while the averaged v value from the pure/LCST fit (0.009 857 L/mol) is close to the value NS fit (0.009 900 L/mol), it is somewhat different from the mixture fit value (0.009 380 L/mol).

Binodal and Spinodal Curves. In Figure 8 the predictions for the spinodal and binodal are compared with experimental data for PS/PVME using the mixture surface parameters (a) and the NS parameters (b). The NS predictions reflect the fact that dPS instead of PS

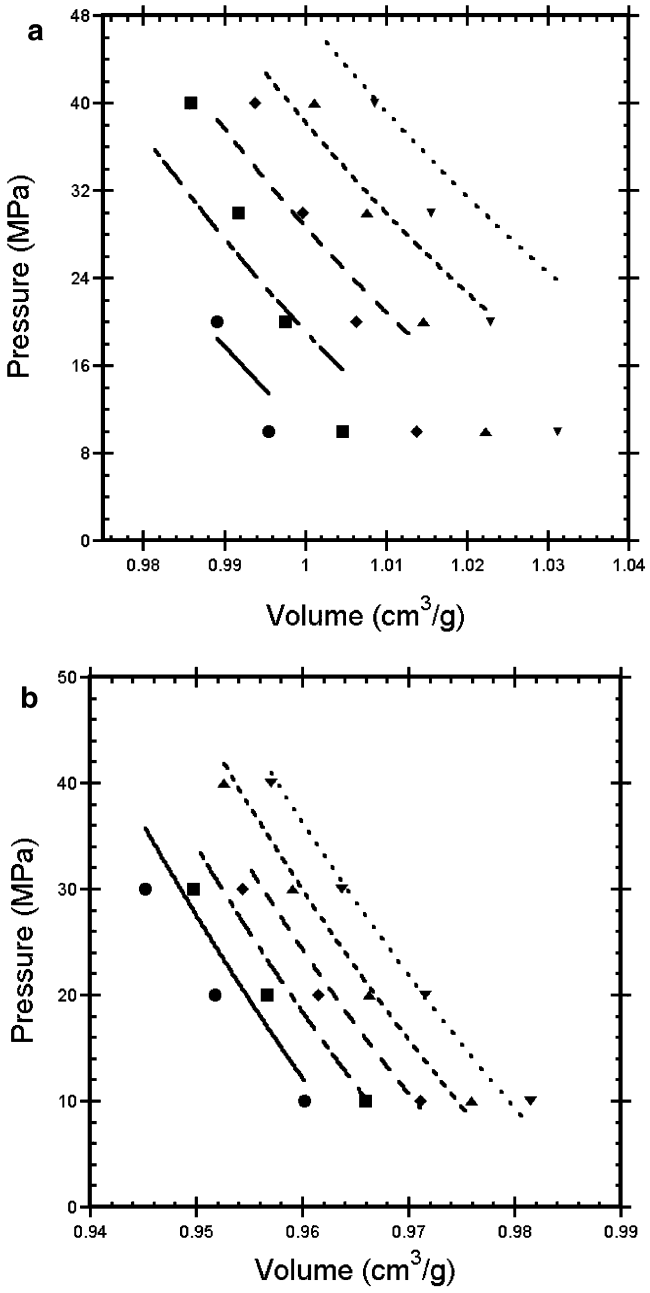

Figure 7. BGY predictions for the PVT behavior of PS/TMPC (a) for the 33% PS surface using the NS fit parameters (b) for the 67% PS surface using the pure/LCST parameters. The symbols represent experimental data.[15]

is used in the blend, a change which results in a shift of roughly 40 K in the LCST. This is illustrated in Figure 8b, which includes the experimental data for the dPS/PVME blend. These two plots may be compared with the BGY fit shown in Figure 5a, which was generated using pure component parameters obtained from fitting pure *PVT* data and g from fitting the critical temperature. In Figure 8, the BGY-generated curves are all predictions. It is clear that the predicted LCST values are in excellent agreement with experimental for both the PS/PVME and the dPS/PVME blend. We also note that the theory predicts a narrowing of the coexistence curve for the dPS blend, compared with the hPS blend, in agreement with what is observed experimentally. The curves predicted in Figure 8a using the parameters from the mixture surface fit are fairly close to those associated with the fit in Figure 5a; however,

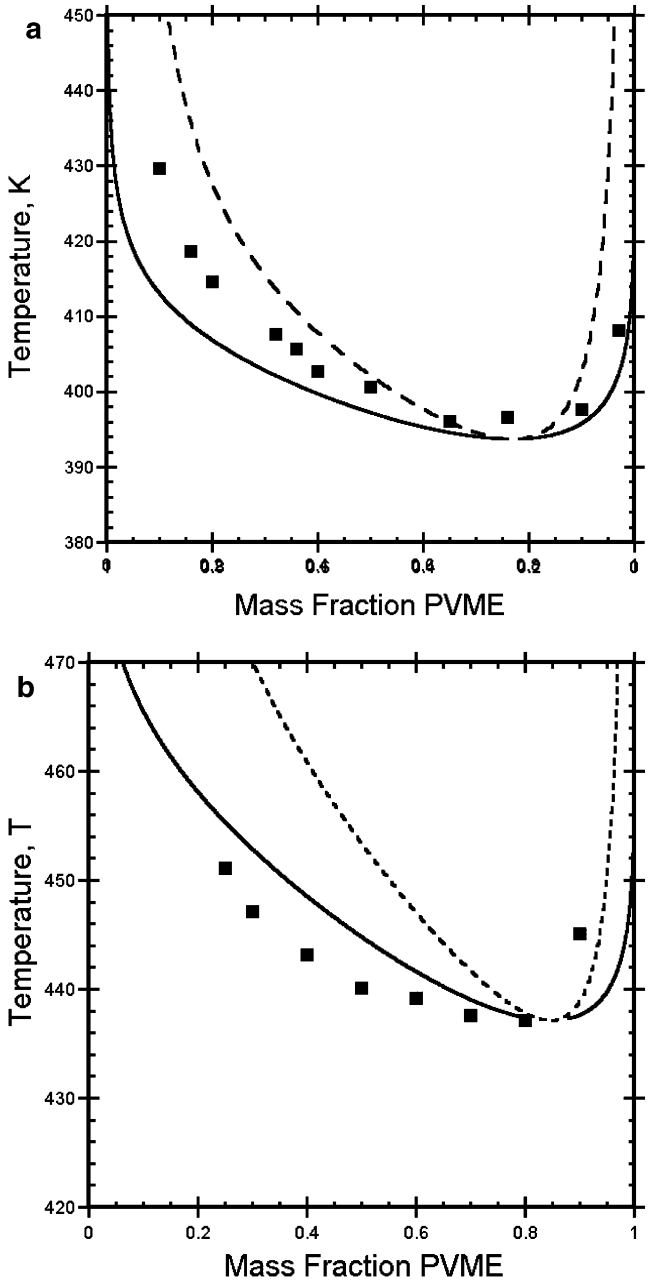

Figure 8. BGY predictions for the PS/PVME LCST, spinodal and binodal using (a) the mixture surface parameters and (b) the NS parameters. In part (a) the data shown are for the hPS/PVME blend,[12] while in part (b) the data shown are for the dPS/PVME blend.[13]

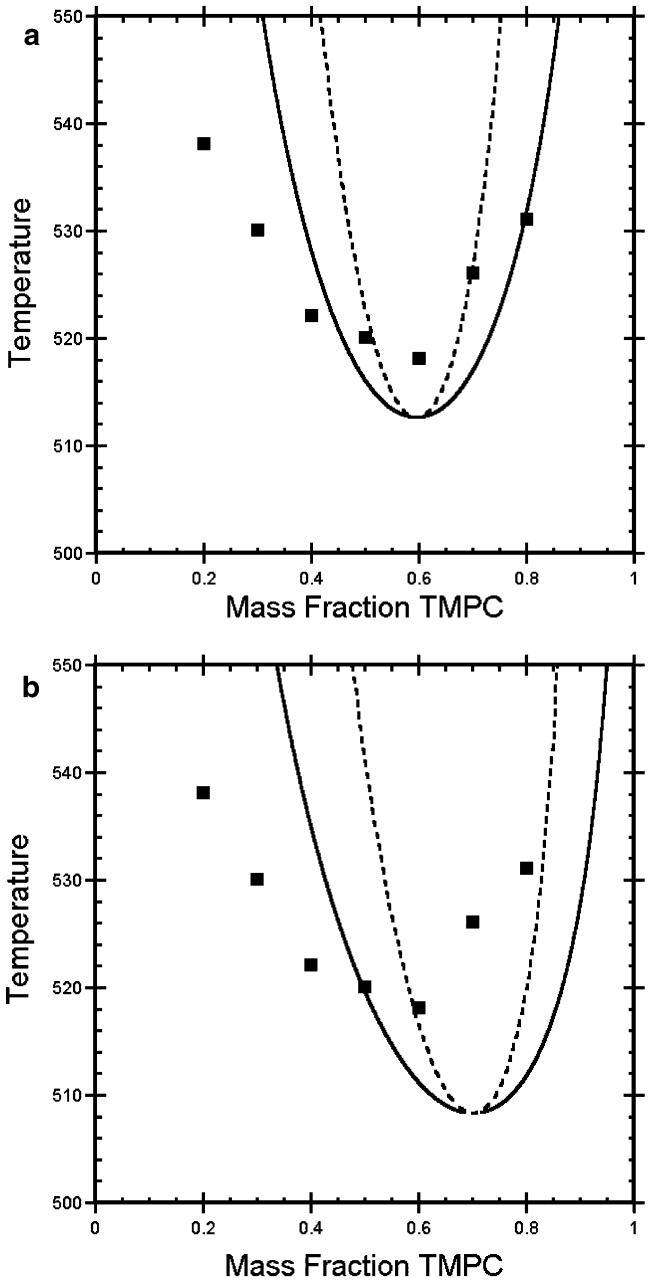

Figure 9. BGY predictions for the PS/TMPC LCST, spinodal and binodal using (a) the mixture surface parameters and (b) the NS parameters. In both plots the experimental data are for the hPS blend.[16]

the predicted critical region is not quite as flat as the experimental points would indicate.

Figure 9 shows the analogous predictions for the PS/TMPC blend, to be compared with the BGY fit to the coexistence data on this blend given in Figure 5b. From the experimental data we see that the PS/TMPC coexistence curve is considerably narrower than that for PS/PVME, and this feature is captured in the BGY predictions. We have observed that, in general, the breadth of the coexistence curve tracks roughly with the absolute difference between the pure component energies. For PS/TMPC this difference is less than half that for PS/PVME, and the curves are correspondingly narrower. In the fit to the LCST shown in Figure 5b the predicted critical composition was slightly too high, and that is also observed in the prediction using the NS parameters, although that using the mixture surface parameters appears to be quite close to the experimental result. Both the mixture surface and the NS parameters underestimate the LCST, the former by about 6 K and the latter by about 10 K, and this is reflected in g values from both these routes which are smaller than that from fitting the LCST. The NS g value does reflect the influence of using dPS, although for the PS/TMPC blend it appears the effect of having dPS in place of hPS is rather modest.[18] The g values for PS/PVME showed a deviation from unity, which was significantly larger than that shown by the g values characterizing the PS/TMPC blend. We observe that as the value of the g parameter deviates further from unity, the calculated binodal and spinodal curves become less sensitive to changes in the g value. For example, if the g parameter starts at a value of 1.001 and undergoes an increase of 0.0005, there is less of an effect on the critical temper-

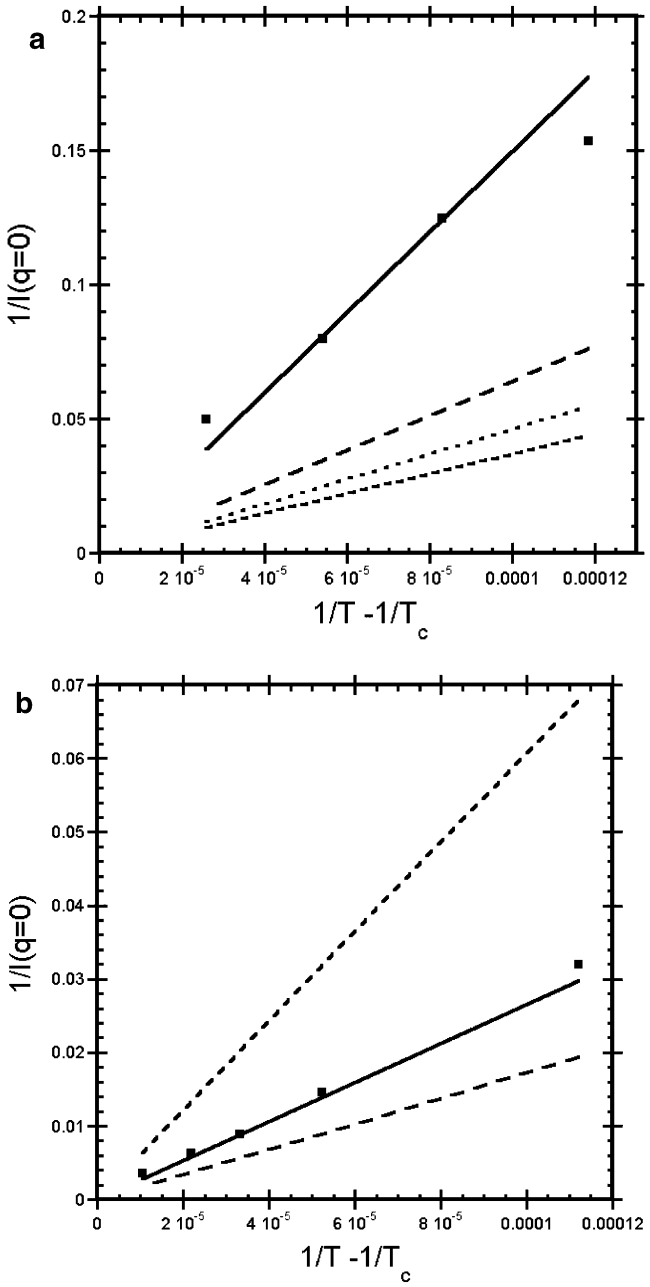

Figure 10. BGY predictions for the inverse zero-angle neutron scattering intensity as a function of inverse temperature (in each of (a) and (b), the solid line represents the fits to experimental data, and the remaining lines are the predictions). (a) For PS/PVME using the mixture surface parameters (long dash), pure/LCST (dPS blend) parameters (dotted), and pure/LCST (hPS blend) short dash. (b) For PS/TMPC using the mixture surface parameters (dotted) and the pure/LCST (hPS blend) parameters (dashed).

ature than if g starts at a value of 1.0001 and undergoes the same increase.

In Figure 10 we compare the experimental NS data with the BGY fit (solid line) as well as with the BGY predictions. As noted before, while the NS data are associated with dPS, most of the other analysis routes do not reflect the effect of deuteration. The sole exception is that we were able to fit to the LCST for dPS/PVME in order to determine g for that blend. However, even in that case the pure component characteristic parameters are needed in order to make any predictions, and those are obtained via data on hPS samples. The predictions shown in Figure 10a therefore involve using the parameters from the mixture surface (long-dashed line), the pure/LCST (for dPS/PVME) (dotted line), and the pure/LCST (for hPS/PVME) (short-dashed line). In Figure 10b the predictions are obtained using the pure/LCST (hPS/TMPC) (dashed line) and mixture surface (dotted line). In both parts of Figure 10 the predicted lines are clearly of different slope than the line fit to experimental data. The trends in slopes and g values appear to be closely correlated, in that larger g values produce larger slopes for both blends, even though the rest of the values in the parameter sets differ for each of the three lines in each plot.

5. Summary

In this work we have developed new routes for the characterization and prediction of blend properties. The method our group and others have commonly used in the past has involved fitting pure component pressure−volume−temperature (*PVT*) data in order to obtain the pure component characteristic parameters and then fitting to a blend critical temperature (upper or lower) in order to determine the mixed interaction parameter; this was called the pure/LCST route. In contrast, the two new methods both involve fitting a relatively smaller set of data on the mixture alone so as to obtain the complete set of parameters, both pure and mixed. The older route makes use of mixture data in one dimension (a critical temperature), while the new routes span two dimensions (neutron scattering data as a function of temperature) or three (mixture *PVT* surface(s)). In the first part of this paper we described using the analytic expressions derived from the lattice BGY theory to fit the experimental data via all three routes. In the second part of the paper we investigated the extent to which each of the methods lead to a thermodynamically consistent picture of the blend. We probed this by using the characteristic parameters obtained by analyzing one set of blend data to predict the remaining two sets of results and then comparing the BGY predictions to experiment. It is useful to recognize that the different experimental routes have different limitations. The "pure/LCST" route involves fitting a mixture temperature, typically associated with a pressure of 0.1 MPa. Neither composition nor pressure dependence is reflected in this datum point. Use of the neutron scattering data ("NS route") involves fitting the inverse zero-angle scattering intensity as a function of temperature. These data were associated with a single composition and a single pressure, again 0.1 MPa. Depending on the system of interest, results at several compositions may be available; we chose to use the more common case in which the available results were limited to one composition. The analysis of the mixture *PVT* surfaces ("mix route") incorporated results for two compositions over a range of both temperature and pressure.

How consistent are the three routes? We found that the predicted results using the three methods were in semiquantitative to quantitative agreement with each other. The largest discrepancy had to do with the mixture *PVT* surface of the PS/PVME blend. In this case, particularly with the 70% PS blend, the presence of the glass transition and the LCST in the temperature range of the *PVT* data resulted in diminished agreement between prediction (using parameters obtained below the LCST and well above the glass transition) and experiment. A separate question has to do with the

agreement between the BGY predictions and the experimental data. This was found to range from good to excellent. We note, in particular, that the theory correctly predicted the experimentally observed narrowing of the coexistence envelope for the d-PS/PVME blend relative to that for the h-PS/PVME blend. In addition, the predictions for the LCSTs of the blends were either identically the experimental values (PS/PVME) or within 6−10 K of experiment (PS/TMPC). We expect there to be some experimental error in the coexistence curve data; however, there is no way for us to quantify the amount.

Overall, the fewest data points are associated with the SANS route, and yet fitting roughly five data points appeared to yield a set of optimized parameters which were just as effective at predicting blend behavior as fitting the many more data points needed for the mixture *PVT* surface. On this basis it is tempting to endorse SANS as the route to follow in characterizing blend thermodynamics. The main drawback here is that we still do not know how to account for the effect of deuteration on the predictions. The closest we could come was in analyzing both the hPS/PVME LCST and the dPS/PVME LCST to find the g factor. While this brought the value of g closer to that obtained by fitting the LCST, it yielded only a partial accounting for the effects of deuteration, as it still did not allow us to determine the difference (if any) in pure component parameters for h-PS compared to d-PS. This is surely an issue in assessing plots in which the predicted and experimental inverse zero-angle scattering as a function of inverse temperature are compared and leads us to believe that it would be valuable to collect *PVT* data on one or more deuterated polymers in order to determine what effect, if any, the deuteration has on pure component properties.

Several trends have appeared in our analysis so far: As the difference between pure component interaction energies increases, the breadth of the coexistence envelope also appears to increase. This difference in energies is roughly 100 J/mol for the PS/TMPC blend and approximately 200 J/mol for PS/PVME. The binodal/spinodal is considerably narrower for the former than the latter. In addition, we note that changing the value of the g factor, which characterizes the difference (through the ratio) of the mixed interaction energy from the geometric mean approximation, causes the value of the critical temperature to shift. The critical temperature also depends on the molar mass of the components, while the critical composition is controlled by the relative molar masses of the two components. For example, in this work we determined the g factor via the pure/LCST route for the PS(110 000)/PVME(99 000) blend to be 1.0017. The g value may be used to make predictions on any other molecular weight PS/PVME blend (although it would likely not apply to oligomeric mixtures). Thus, for a PS(67 000)/PVME(95 000) blend we predict a critical temperature of 404.5 K and a critical composition of 0.51 weight fraction PVME, which compares well with the experimental result of 403 K and 0.5 PVME.[24] Note that the critical composition has shifted to lower PVME weight fraction relative to the value of about 0.7 weight fraction for the higher molecular weight blend we originally studied.

In terms of correlations with g, we also found that for each of the blends the ordering of the plots of inverse scattering intensity as a function of inverse temperature correlated with the value of g, the largest value of g being identified with the plot having the largest slope. However, it is difficult to interpret the relative ordering associated with the different methods of analysis since, as noted above, we still do not yet understand the influence of deuteration on the value of g.

The literature is sprinkled with efforts to make predictions on blend properties by using experimental data on the pure components along with some means of accounting for the mixed interaction without having to analyze data on the mixture itself. Indeed, some of us have contributed to such efforts. Having analyzed a variety of blends, including the ones studied here, we believe that such a route is likely to produce rather narrowly defined successes. Accurate prediction of the free energy of mixing means finding the correct balance between a very small energy and a similarly small (temperature times) entropy of mixing. Thus, to account for partial miscibility, one is hostage to what are often exquisitely minute deviations in the mixed interaction energy relative to the geometric mean approximation. On the basis of the results described here, we would like to suggest an alternate way of proceeding. Through the use of one of the new routes we have outlined in this paper it is possible to bypass altogether the collection of pure component data and focus entirely on a relatively modest set of data on the mixture. In this work we have used mixture *PVT* data and zero-angle scattering intensities as a function of temperature. In the former case we made use of results for two compositions; however, qualitatively similar conclusions can be drawn if only one *PVT* surface (for a single composition) is analyzed. The data requirement using SANS results is even more sparse: one composition, atmospheric pressure, and as few as five data points. Analysis of either data set leads to a complete set of both pure and mixed characteristic parameters which yield predictions for blend behavior over a range of composition, temperature, and pressure which are in good to superb agreement with experimental results. In addition, we have found that the resulting pure component parameters may be used effectively in predicting pure component *PVT* surfaces. Consideration of alternative routes to the equation of state properties for pure components will be the subject of a future paper.

Acknowledgment. The authors appreciate the financial support they have received in undertaking this research: NSF-DMR-0099541 (J.E.G.L.), EPSRC (J.S.H. and J.E.G.L.), and GAANN (M.T.). J.E.G.L. also very much appreciated the hospitality of those in the Chemical Engineering and Technology Department at Imperial College, where some of this research was carried out. The authors also thank J. T. Cabral for the use of his detailed neutron scattering results on the PS/TMPC blend which were used in this analysis.

References and Notes

(1) Lipson, J. E. G. *Macromolecules* **1991**, *24*, 1334.
(2) Sevian, H. M.; Brazhnik, P. K.; Lipson, J. E. G. *J. Chem. Phys.* **1993**, *99*, 4112.
(3) Lipson, J. E. G. *Macrmol. Theory Simul.* **1998**, *7*, 263.
(4) Taylor, M. P.; Lipson, J. E. G. *J. Chem. Phys.* **1998**, *109*, 7583.
(5) Lipson, J. E. G.; Andrews, S. S. *J. Chem. Phys.* **1992**, *96*, 1426.
(6) Luettmer-Strathmann, J.; Lipson, J. E. G. *Phys. Rev. E* **1999**, *59*, 2039.
(7) Lipson, J. E. G.; Tambasco, M.; Willets, K. A.; Higgins, J. S. *Macromolecules* **2003**, *36*, 2977.

(8) Flory, P. J. *Principles of Polymer Chemistry;* Cornell University: Ithaca, NY, 1953.
(9) Guggenheim, E. A. *Proc. R. Soc. London, Ser. A* **1944**, *183*, 203.
(10) Sanchez, I. C.; Lacombe, R. H. *Macromolecules* **1978**, *11*, 1145.
(11) Panayiotou, C.; Vera, J. H. *Polym. J.* **1982**, *14*, 681.
(12) Zoller, P.; Walsh, D. J. *Standard Pressure−Volume−Temperature Data for Polymers;* Technomic Pub. Co.: Lancaster, PA, 1995.
(13) Beaucage, G.; Stein, R. S.; Hashimoto, T.; Hasegawa, H. *Macromolecules* **1991**, *24*, 3443.
(14) Beaucage, G.; Stein, R. S.; Koningsveld, R. *Macromolecules* **1993**, *26*, 1603.
(15) Yang, H.; Shibayama, M.; Stein, R. S.; Shimizu, N.; Hashimoto, T. *Macromolecules* **1986**, *19*, 1667.
(16) Jeon, K. S.; Char, K.; Walsh, D. J.; Kim, E. *Polymer* **2000**, *41*, 2839.
(17) Kim, C. K.; Paul, D. R. *Polymer* **1992**, *33*, 1630.
(18) Cabral, J. T. Doctoral Thesis, Imperial College, London.
(19) Cabral, J. T.; Higgins, J. S.; McLeish, T. C. B.; Strausser, S.; Magonov, S. N. *Macromolecules* **2001**, *34*, 3748.
(20) Tompa, H. *Polymer Solutions*; Butterworth: London, 1956.
(21) Higgins, J. S.; Benoit, H. C. *Polymers and Neutron Scattering*; Oxford Science Publications: Oxford, 1994.
(22) Rowlinson, J. S.; Swinton, F. L. *Liquids and Liquid Mixtures,* 3rd ed.; Butterworth: London, 1982.
(23) Luettmer-Strathmann, J.; Schoenhard, J. A.; Lipson, J. E. G. *Macromolecules* **1998**, *31*, 9231.
(24) Walsh, D. J.; Dee, G. T.; Halary, J. L.; Ubiche, J. M.; Millequant, M.; Lesec, J.; Monnerie, L. *Macromolecules* **1989**, *22*, 3395.

MA048647H